

Article

A Novel 12-Lead ECG T-Shirt with Active Electrodes

Anna Boehm *, Xinchu Yu, Wilko Neu, Steffen Leonhardt and Daniel Teichmann

Philips Chair for Medical Information Technology, RWTH Aachen University, Pauwelsstr. 20, 52074 Aachen, Germany; yu@hia.rwth-aachen.de (X.Y.); wilko.neu@rwth-aachen.de (W.N.); leonhardt@hia.rwth-aachen.de (S.L.); teichmann@hia.rwth-aachen.de (D.T.)

* Correspondence: boehm@hia.rwth-aachen.de; Tel.: +49-241-80-23224

Academic Editors: Enzo Pasquale Scilingo and Gaetano Valenza

Received: 13 August 2016; Accepted: 3 November 2016; Published: 8 November 2016

Abstract: We developed an ECG T-shirt with a portable recorder for unobtrusive and long-term multichannel ECG monitoring with active electrodes. A major drawback of conventional 12-lead ECGs is the use of adhesive gel electrodes, which are uncomfortable during long-term application and may even cause skin irritations and allergic reactions. Therefore, we integrated comfortable patches of conductive textile into the ECG T-shirt in order to replace the adhesive gel electrodes. In order to prevent signal deterioration, as reported for other textile ECG systems, we attached active circuits on the outside of the T-shirt to further improve the signal quality of the dry electrodes. Finally, we validated the ECG T-shirt against a commercial Holter ECG with healthy volunteers during phases of lying down, sitting, and walking. The 12-lead ECG was successfully recorded with a resulting mean relative error of the RR intervals of 0.96% and mean coverage of 96.6%. Furthermore, the ECG waves of the 12 leads were analyzed separately and showed high accordance. The P-wave had a correlation of 0.703 for walking subjects, while the T-wave demonstrated lower correlations for all three scenarios (lying: 0.817, sitting: 0.710, walking: 0.403). The other correlations for the P, Q, R, and S-waves were all higher than 0.9. This work demonstrates that our ECG T-shirt is suitable for 12-lead ECG recordings while providing a higher level of comfort compared with a commercial Holter ECG.

Keywords: ECG; unobtrusive measurement; wearables

1. Introduction

Unobtrusive sensing of vital signs, such as cardiac activity and respiration, has been increasingly applied in the past decade. The aging of our society has resulted in an increasing demand on medical staff, which cannot always be met. As a result, an increasing number of technical solutions, the so-called personal healthcare systems, are being developed. They aim at enabling sick and elderly patients to stay at home for a longer period, rather than facing prolonged hospital stays. When staying at home, patients generally benefit from increased comfort, which may accelerate their recovery. In turn, costs for the healthcare system will be reduced by shortening the stay in hospital. This is the main rationale for developing long-term monitoring solutions for the home environment.

One of the established long-term cardiac monitoring devices is the Holter. This is a portable electrocardiography (ECG) device with up to 12 leads for long-time application. These ECG recorders are often used to diagnose cardiac conditions over the duration of several days. For this, patients wear the device while continuing their daily routine.

Commercial Holter devices consist of a portable ECG recorder with adhesive electrodes. However, these electrodes have one major problem: the gel that ensures good conductivity can lead to skin allergies. Moreover, the longer the gel is applied, the greater the possibility that more problems arise. Signal quality is deteriorated if the gel dries up, which is highly probable during long-term monitoring. In addition, in some cases (e.g., if patients are sweating), the electrodes detach themselves, requiring reapplication. If this occurs, the patient may not reattach them in the correct

place. In order to address these problems and to improve patient comfort, we developed a 12-lead ECG T-shirt with active electrodes and a portable ECG recorder.

Various textile ECG T-shirts have been investigated in the last decade. Whereas some systems were developed mainly for research purposes only [1–4], some shirts are commercially available: CardioLeaf (Clearbridge VitalSigns, Singapore) and hWear (HealthWatch Technologies, Kfar Saba, Israel) [5,6]. The latter type is a shirt that is compatible with a 12-lead ECG recorder.

Furthermore, textile electrodes have been used for ECG acquisition in research [7–12]. It was discovered that certain dry textile electrodes can achieve comparable results to conventional electrodes in resting electrocardiography but have lessened signal quality during movement [13]. However, most dry electrodes have very high contact impedances to the skin. To improve signal quality, active circuits with buffers are used on the electrodes, forming an active electrode. An active electrode is comprised of a sensing part (conductive textile), front-end electronics and shielding [14]. The input impedance is very high and the output impedance is low. The output can drive a long screened cable, reducing the power line interference and cable movement.

The principle of active electrodes has been widely applied for capacitive ECGs and can be found in multiple systems, such as ECG chairs [15], car seats [16], beds [17–20], toilet seats [21], a bathtub [22], and clothing [8,9].

Because none of the commercially available ECG T-shirts were compatible with our design for active electrodes, we developed a custom T-shirt with 10 electrodes. The electrode material is an electrically conductive fabric sewn into the inside of a sports T-shirt. Our T-shirt does not require electrode gel. Furthermore, it can be worn as an undergarment. The T-shirt is attached to a (relatively small) hand-held ECG recording device.

This article is structured as follows: first, we describe the design of the measurement system and the experimental design. This is followed by the results, the experimental data, a discussion of the results, and, lastly, conclusions are presented.

2. Materials and Methods

The portable 12-lead ECG measurement system consists of a T-shirt, active electrodes and an ECG recorder. The active electrodes of the capacitive measurement system record the potentials on the body's surface. The analogue signals from the active electrodes are digitalized in the ECG recorder, which also calculates the 12 ECG leads. The signals of the leads are then processed by a microcontroller and stored on an SD card in the ECG recorder. In terms of practicability, it would have been an option to send the data wirelessly. The two main reasons why no wireless module was used are medical data protection and power consumption. A wireless module would drastically reduce battery life, especially when sending data of 12 channels at a high sample rate.

2.1. 12-Lead ECG

A 12-lead ECG requires 10 electrodes on the patient's limbs and chest: 10 physical channels are recorded (3 limb leads, 6 thoracic leads, 1 RL lead), as shown in Figure 1.

In Holter ECGs, the electrodes are placed only on the chest. Figure 1 shows that, additional to the 3-lead setup for Einthoven and Goldberger, 6 Wilson leads are included. Einthoven and Goldberger leads are calculated from three electrodes forming a triangle, namely the left leg (LL), left arm (LA) and right arm (RA), also called limb electrodes. The fourth electrode applied is the neutral or right leg electrode. The bipolar Einthoven leads are calculated as follows:

$$I = LA - RA, \quad (1)$$

$$II = LL - RA, \quad (2)$$

$$III = LL - LA, \quad (3)$$

so that $III = II - I$.

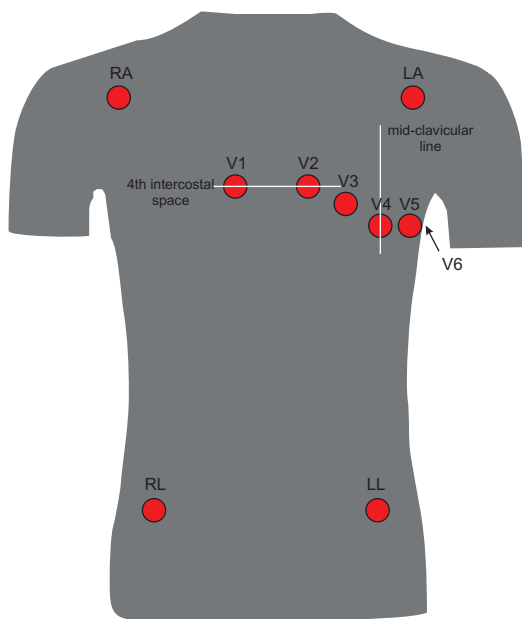


Figure 1. Positions of the 12-lead electrocardiograph (ECG).

The regular shape of the Einthoven II lead is shown in Figure 2. The ECG can be divided into different waves that are referred to as P to T. They reflect the stages of the electrical excitation propagation of the heart. The P-wave is the depolarization of the atria. The QRS complex (QRS waves) reflects the depolarization of the ventricles and the T-wave is their repolarization.

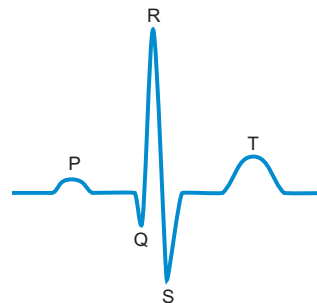


Figure 2. ECG morphology.

The unipolar Goldberger leads are also recorded for the 12-lead ECG. The Goldberger leads, denoted aVR, aVL and aVF, are augmented leads. These leads are formed using an augmented reference electrode, which is a combination of the two other limb electrodes. This is calculated as follows:

$$aVR = RA - \frac{1}{2}(LA + LL), \quad (4)$$

$$aVL = LA - \frac{1}{2}(RA + LL), \quad (5)$$

$$aVF = LL - \frac{1}{2}(RA + LA). \quad (6)$$

The Wilson leads are placed around the left side of the rib cage. Wilson leads are used to detect local irregularities of electric cardiac function, such as infarctions. The leads are labeled V1 to V6. Their reference is called the Wilson central terminal (WCT). It is a reference potential that is formed by connecting all three limb electrodes to 5 k ohm resistors resulting in their average [23].

2.2. Measurement System

2.2.1. T-Shirt

The T-shirt is a commercially available breathable sports T-shirt (Nike Legend Pro DRI-FIT, Beaverton, OR, USA). Ten textile patches made of electrically conductive fabric (Shieldex Med-tex P180, Statex, Bremen, Germany) serve as electrodes. The patches ($4\text{ cm} \times 4\text{ cm}$) are sewn into the interior of the T-shirt (see Figure 3). This fabric is silver plated with 99% silver and has been used as electrodes by two other groups [24,25]. While other conductive textile materials exist, silver coating was selected. It was found that silver electrodes are advantageous even at recording low frequencies [26].

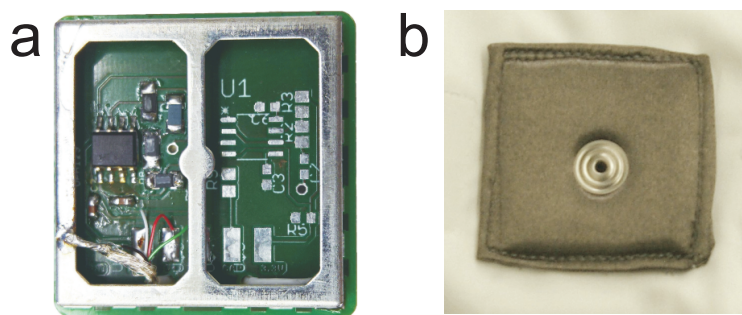


Figure 3. Active electrode. (a) active circuit printed circuit board (PCB); and (b) textile electrode on the interior of the T-shirt.

The locations are chosen according to the common 12-lead ECG setup (see Figure 1). The driven right leg (DRL) electrode has a larger area to ensure good contact ($30\text{ cm} \times 5\text{ cm}$). Each electrode has a snap fastener connection, where the amplifier boards (or in the case of the DRL electrode, the cable) that lead to the ECG recorder are fastened.

The T-shirt needs to fit relatively tightly, since signal quality improves with contact pressure of the electrodes. Therefore, we added a few Velcro straps to “tighten” the T-shirts and keep the electronics in place.

2.2.2. Electrodes

The textile electrodes are followed by active circuits. The aim was to improve the signal quality of a dry or an optionally capacitive setup.

The main principle of the active electrodes is shown in Figure 4. As mentioned, the textile patches serve as electrodes and they are connected to the outside of the T-shirt by snap fasteners. An active circuit PCB is placed on the snap fasteners from the exterior.

More precisely, an impedance converter with OPA129U (Texas Instruments, Dallas, TX, USA) on the PCB decouples the ECG signal at the snap fastener from the following electronics. A highly resistive bias resistor (10 G ohm) prevents the build-up of static charge at the input on the impedance converter. Then, the analogue output of the impedance converter is led to the ECG recorder with a shielded six-wire cable. This cable also carries extra wires for the power supplies (see Figure 3).

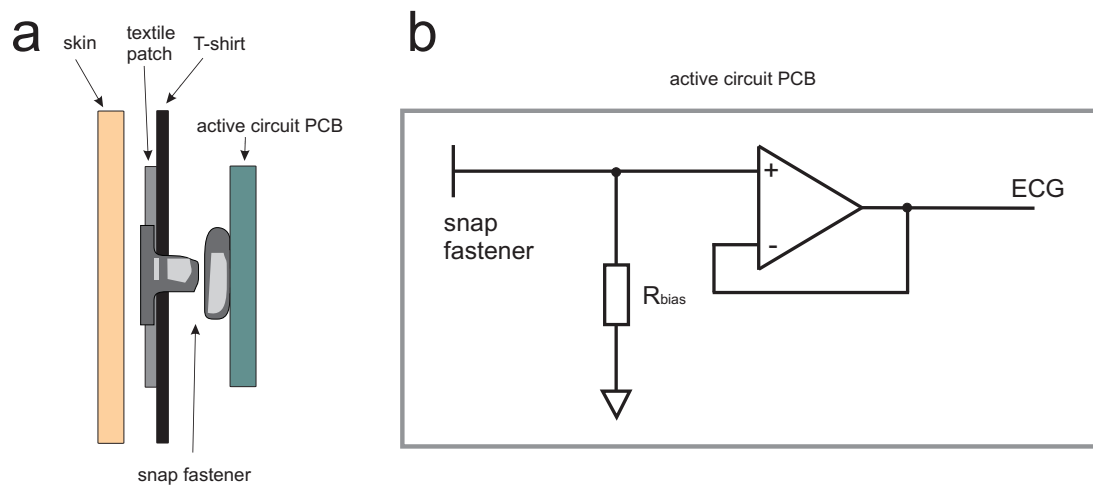


Figure 4. Electrode principle. (a) structure of the connection of the skin to the electrodes on the T-shirt; and (b) simplified diagram of an active electrode circuit.

The tenth electrode is the so-called DRL electrode, which attenuates common mode signals and produces a better signal-to-noise ratio. The DRL signal is generated in the ECG recorder on an integrated chip and is fed into the electrode patch of the right leg. The T-shirt and the active electrodes are presented in Figure 5.

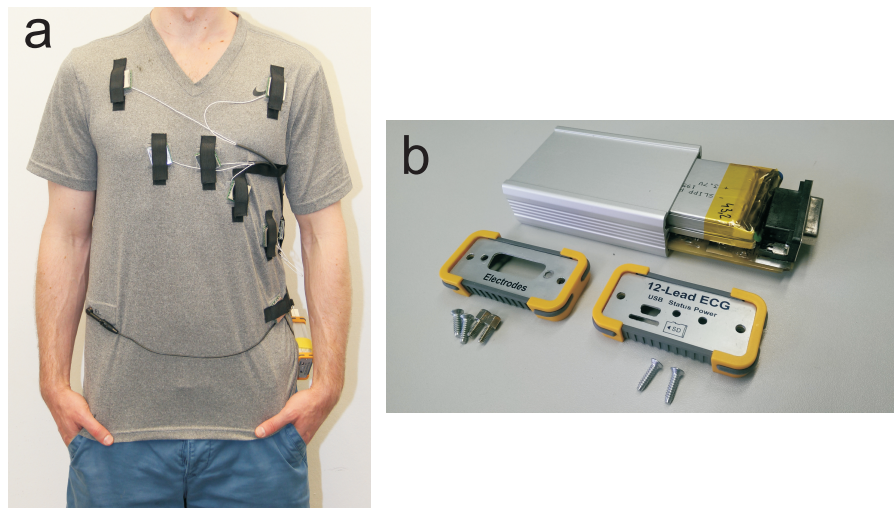


Figure 5. (a) ECG T-shirt with electrodes; and (b) ECG recorder.

2.2.3. 12-Lead ECG Recorder

The 12-lead ECG recorder is a portable device with the following dimensions: 70 mm × 65 mm × 30 mm (Figure 5) and weighs 180 g.

Figure 6 presents details of the recorder. The design is based on two ADS1298 analogue digital converters (ADC) (Texas Instruments, Dallas, TX, USA). The ADS1298 chip is a designated ECG ADC converter. It has eight differential ADC input channels with 24-bit resolution and a sample rate that can be set from 250 samples per second (SPS) to 32,000. It also has the capability of calculating the 12-lead ECG and a DRL signal.

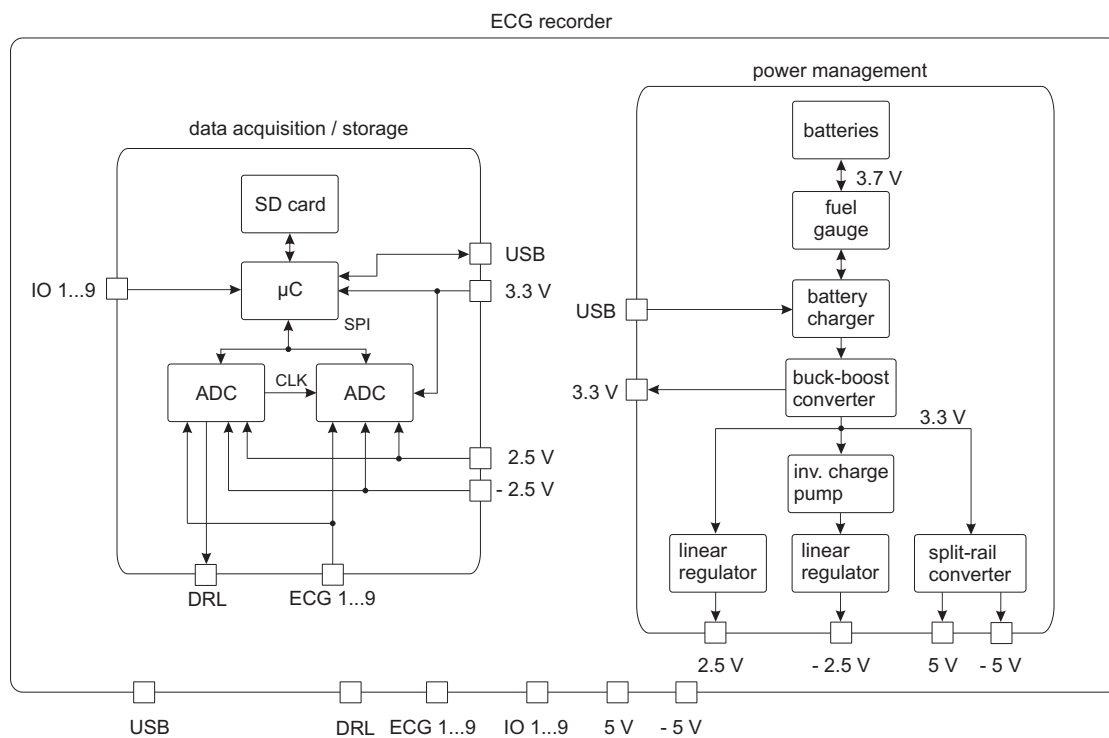


Figure 6. Complete block diagram of the ECG recorder.

As our design consists of two ADS1298, 16 channels are available and a true 12-lead ECG can be recorded. This means that the 12-lead ECG is recorded with 10 electrodes and is not estimated from a smaller number of electrodes. Both chips are connected in parallel to one serial peripheral interface (SPI) port of the microcontroller using separate chip select (CS) lines (see Figure 7). One of the ADS1298 is the master and provides its clock for synchronization and the other is the slave. They are started with a START signal. The ADS1298 signals the microcontroller when data are available and ready to be sent. Since both ADS1298 are synchronized, data from both chips can be retrieved. After retrieving data from the first chip, the CS line is switched and the second one is read out. The sampling rate is set to 500 SPS ; no other sampling rates are used.

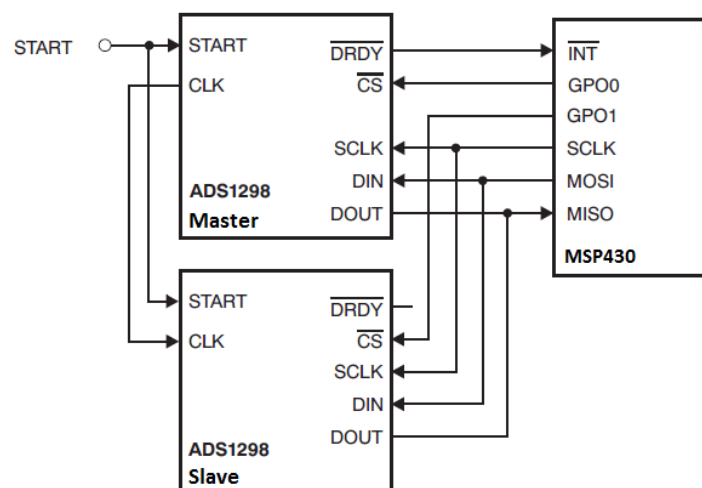


Figure 7. Diagram of the master and slave ADS1298 with the microcontroller.

The ADS1298 has differential inputs that can be enhanced by a gain factor. The bipolar Einthoven leads II and III are recorded on the master ADS1298 by the differences of its respective electrodes (see Equations (1)–(3)). The Wilson Central Terminal (WCT) is generated internally using the three limb leads. In addition, a DRL circuitry is on board the ADS1298 using the WCT signal.

The second ADS1298 is primarily used to generate the Goldberger leads and to record the Einthoven lead I. The augmented leads are created according to Equations (4)–(6). The reference is formed by averaging the other two limb electrode potentials. Because only five of the eight channels are used for Goldberger, the three remaining channels can be used for other sensors.

A microcontroller MSP430F5529 (Texas Instruments, Dallas, TX, USA) was used. This microcontroller has low power consumption, but is fast enough to write on a micro SD with 200,000 bytes/s. Additionally, the MSP430F5529 has an SPI to access the ADS1298 and to store the ECG data onto the microSD, with up to 64 GB storage.

In order to run a portable device, the power is provided by two 3.7 V rechargeable lithium polymer batteries with 1950 mAh and 1400 mAh, respectively. Two different sizes of batteries were chosen to enable a perfect fit into the small casing. Power management had to be devised carefully, since not only the internal components of the ECG recorder require power, but also the active electrodes. Moreover, as the system is intended for long-time recording purposes, battery life is an important issue.

A safety circuit uncouples the battery if the voltage of the cells is below 2.7 V. A fuel gauge BQ27441 (Texas Instruments, Dallas, TX, USA) is used to estimate the remaining battery capacity and the state of charge. The batteries are charged via a mini USB connector on the recorder with an external power source. The loading of the batteries is solved with a BQ24075 (Texas Instruments, Dallas, TX, USA) chip, which can load with up to 1.5 A current and is set to 1.317 A. Charging begins as soon as the USB port is connected.

Several power sources are required. The microcontroller needs a constant voltage supply of 3.3 V, which is provided by a TPS63030 (Texas Instruments, Dallas, TX, USA) buck-boost converter. The two ADS1298 are supplied by a symmetrical power supply of ± 2.5 V, which is generated by TPS799 (Texas Instruments, Dallas, TX, USA) and the TPS723 (Texas Instruments, Dallas, TX, USA) negative output linear regulator. It also needs 3.3 V digital supply.

The OPA129U chip of the active electrodes requires a minimum of ± 5 V. Other than with conventional wet electrodes, higher baselines can occur; therefore, the higher power supply would be beneficial to avoid saturation of the amplifier through DC offsets. However, only ± 5 V was chosen. This improves battery running time and satisfies the concerns about patient safety. This ± 5 V power source was implemented by using the TPS65131 (Texas Instruments, Dallas, TX, USA) split-rail converter, which has a positive and negative voltage output. In total, around 260 mW are needed for recording, which leads to an estimated maximum runtime of 47 h.

2.3. Measurement Setup

The design was experimentally tested on three healthy male volunteers. The subjects were asked to wear both the 12-lead ECG T-shirt and the reference Holter ECG BT12 (Corscience, Erlangen, Germany) at the same time. The BT12 has a software that displays the ECG channels and the heart rate in real-time. However, only raw data that can be exported from the software, which does not include the RR (beat-to-beat) or heart rate information. Data collection with the ECG T-shirt hardware is as follows: after a recording is started, the data is stored on the SD card in the recorder. The raw data can then be transferred to a PC for further processing.

Three experimental scenarios were conducted for 5 min each: (i) lying in bed; (ii) sitting; and (iii) walking at 1.49 mph. We hypothesized that whilst lying down, fewer movement artifacts would occur than during the other two scenarios. In addition, heart rate at rest was expected to be lower compared with sitting and walking.

The data were post-processed on a PC with an Intel Core i5-2500 CPU @ 3.30 GHz (Intel Corporation, Santa Clara, CA, USA) and 8 GB RAM. The first step was to filter the obtained

ECG data with a 3rd order Butterworth bandpass filter between 2 and 20 Hz. In order to obtain the RR intervals (beat-to-beat intervals), a method for beat-to-beat interval identification of multi-channel data based on self-similarity features was applied for the reference and T-shirt data [27]. Using this method, beat-to-beat intervals in any kind of cardiac-related data can be determined as long as a repetitive pattern is detectable. In this way, the RR intervals of the shirt and the reference were calculated.

The data of the two systems had to be synchronized, since the devices could not be started at exactly the same time. The idea was to make use of heart rate variability. Every healthy person has a slight variation in heart rate over time and, thus, a variation in RR intervals. This fact was used to match both systems by aligning intervals of the same length.

For that, a prominent sequence, which appears in the intervals of both the T-shirt ECG and the reference ECG, was manually selected (see the vertical dotted lines in Figure 8).

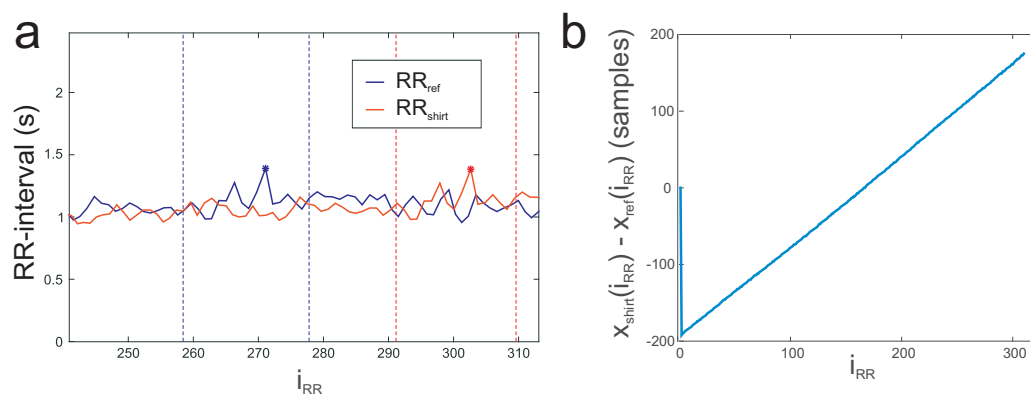


Figure 8. (a) synchronization using RR intervals; and (b) the difference between corresponding samples $x_{\text{shirt}}(i_{\text{RR}}) - x_{\text{ref}}(i_{\text{RR}})$ rises linearly.

Afterwards, the respective maximum was automatically detected in each of the two sequences (see markers in Figure 8). Finally, the time shift was automatically computed using the difference between the two maximums, and the timestamps of the T-shirt ECG and the reference ECG were corrected accordingly.

However, the data did not yet correspond because the sampling rates of the devices were slightly off. Despite the sampling rate of $f_s = 500$ Hz, the data did not correspond. Therefore, the next step was to determine the samples $x_{\text{ref}}(i_{\text{RR}})$ and $x_{\text{shirt}}(i_{\text{RR}})$ of the corresponding intervals $i_{\text{RR}} = \{1, 2, \dots, m\}$ and to calculate their difference $\Delta x = x_{\text{shirt}} - x_{\text{ref}}$. This difference increases linearly over the course of the measurement, as can be seen in Figure 8. This linearity was used to approximate a function $\Delta x = p_1 \cdot x_{\text{shirt}} + p_0$. The mean was $p_0 = 0.0025$ and $p_1 = -296.16$. We adjusted the time stamps of the commercial device by adding $\Delta x / f_s$. This was calculated for every measurement separately. The ECG data were matched with the new time base and could then be adequately compared. Mathematical modeling was only done for the purpose of evaluation and for the comparison of our system to the reference system. In future, the reference system is not intended for the use at the same time.

3. Results

The experimental data obtained from the novel device were analyzed. Extracted RR intervals as well as the morphology of the ECG wave were compared with the reference signal.

3.1. RR Interval Analysis

The relative error for the RR intervals was computed for all three scenarios with all subjects. The duration of each experiment was 5 min. The relative error and signal coverage (percentage of the entire measurement time during which the signal was evaluable) were computed (Table 1). In one

experiment (S1 walking), the ECGs were exceptionally noisy: the coverage was only 49.5% with a relative error of 75.5%. This particular measurement was disregarded for further analysis. The mean relative error for the RR intervals in every scenario was 0.96% and the mean coverage of the signal was 96.6%.

Table 1. Relative error of RR intervals and coverage for RR interval determination.

Subject	Scenario	Relative Error	Coverage	Duration (s)	Beats
S1	lying	0.0024	0.9942	314.75	305
S1	sitting	0.0022	0.9939	296.31	344
S1	walking *	0.755	0.4952	350.01	468
S2	lying	0.0022	0.9775	295.90	284
S2	sitting	0.0029	0.9898	297.54	323
S2	walking	0.0031	0.9938	290.57	368
S3	lying	0.0216	0.8881	300.82	295
S3	sitting	0.0208	0.949	296.31	305
S3	walking	0.0218	0.9449	296.31	365
Mean		0.0096 *	0.9664 *	304.28	340

* S1 walking was excluded from the mean.

The Bland–Altman diagram for all subjects is presented in Figure 9; the RR intervals extracted from both devices are compared in this diagram. The RR intervals used in this section were extracted from the Einthoven II lead with the algorithm by Brueser [27]. Furthermore, only artifact-free data were selected for the diagram, so the mean coverage was 87.2%. The bias was at -1.9 ms and the 95% limits of agreement were -20.1 ms and -23.9 ms.

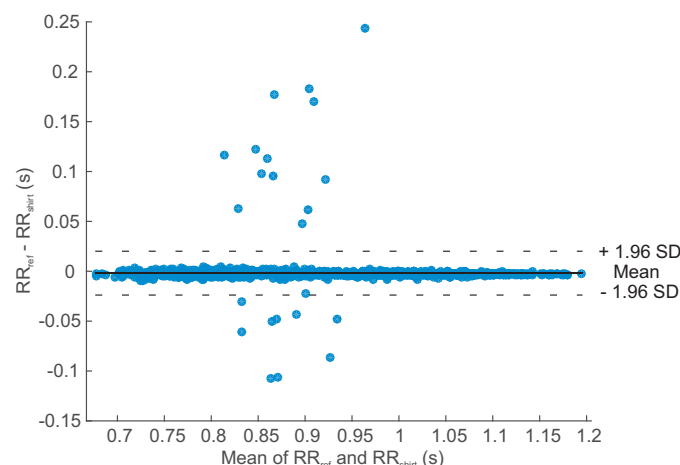


Figure 9. Bland–Altman diagram. The bias is at -1.9 ms, whereas the 95% limits of agreement are at -20.1 ms and -23.9 ms, respectively. The solid line indicates the bias/mean difference and the dashed lines indicate the 95% of limits of agreement. The mean coverage was 87.2%. S1 walking was excluded.

3.2. ECG Wave Analysis

In addition to RR interval analysis, the ECG leads were segmented into their P, Q, R and S-waves. Data with artifacts were selected manually and subsequently discarded. Finally, the resulting ECG waves were compared. For that purpose, a script was written to automatically identify the R, P, Q and S-waves. Since the location of the R-wave is easily found, the other waves could be identified as peaks relative to that position.

Figure 10 shows an excerpt from the Einthoven II lead from subject S1. The data of the T-shirt and the reference were bandpass-filtered (2–20 Hz) beforehand. The waves are highlighted for both ECG curves. The R-peaks of the lead and the other waves correspond.

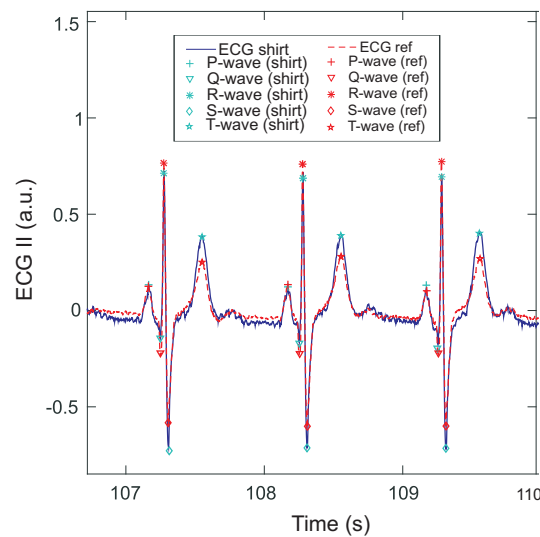


Figure 10. Exemplary comparison of Einthoven lead II from S1 (lying), bandpass filtered (2–20 Hz) from ECG T-shirt and reference.

Next, a closer analysis of the P, Q, R and S-waves was performed. Tables 2–4 present the results for the three scenarios: lying, sitting and walking. The temporal correlation of the data from both devices was calculated for each wave separately using Pearson's linear correlation coefficient. For each wave, the time stamp of the prominent peak was correlated. The mean correlation of each wave per lead is shown in Tables 2–4. The correlation signifies the matching of the waves extracted from both devices. A correlation close to zero indicates poor correspondence of the signals, whereas a correlation close to 1 indicates high correspondence. Additionally, the median of the time differences $t_{\text{shirt}}(i_{\text{wave}}) - t_{\text{ref}}(i_{\text{wave}})$ for the occurrence $i_{\text{wave}} = \{1, 2, \dots, n\}$ are determined for each P, Q, R and S wave per lead. These values indicate the time difference of the estimated waves in ms. A difference close to 0 ms is a perfect match. If this value is higher, the match is less precise.

Table 2. Data on statistics of all subjects (lying) with coverage: $86.79\% \pm 4.13\%$. Mean correlation and median of time difference ($t_{\text{shirt}} - t_{\text{ref}}$) for all subjects for P, Q, R, S, and T waves.

Lead	Correlation					Difference (ms)				
	P	Q	R	S	T	P	Q	R	S	T
I	0.900	0.952	0.957	0.957	0.762	2	10	2	-4	-2
II	0.879	0.957	0.957	0.957	0.957	2	0	2	2	-2
III	0.939	0.957	0.957	0.958	0.882	2	2	2	4	0
aVR	0.947	0.957	0.957	0.957	0.863	0	-2	2	0	8
aVL	0.871	0.953	0.957	0.953	0.732	26	2	2	14	-50
aVF	0.942	0.957	0.957	0.958	0.807	2	2	2	2	4
V1	0.952	0.955	0.957	0.954	0.706	2	4	2	-4	4
V2	0.943	0.957	0.957	0.955	0.826	2	2	2	0	12
V3	0.936	0.956	0.957	0.957	0.875	-2	0	2	-2	22
V4	0.917	0.957	0.957	0.957	0.757	0	4	2	4	6
V5	0.892	0.957	0.957	0.957	0.787	0	4	2	4	8
V6	0.920	0.957	0.957	0.958	0.850	0	4	2	6	8
Mean	0.920	0.956	0.957	0.957	0.817	3	3	2	2	2

For lying down, the data of all subjects were evaluable and the overall coverage was $86.79\% \pm 4.13\%$. Mean correlation was $92.14\% \pm 6.05\%$ and the time difference was 2.4 ± 0.5 ms.

For sitting, the ECG data of all subjects were evaluable and the overall coverage was $94.37\% \pm 3.3\%$. Mean correlation was $91.1\% \pm 11.55\%$ and the time difference was 0.6 ± 10.9 ms.

For walking, the ECG data of only subjects S2 and S3 were acceptable and the overall coverage was $83.47\% \pm 5.09\%$. Mean correlation was $76.9\% \pm 22.39\%$ and the time difference was 6.6 ± 14.7 ms.

Table 3. Data on statistics of all subjects (sitting) with coverage: $94.37\% \pm 3.30\%$. Mean correlation and median of time difference ($t_{\text{shirt}} - t_{\text{ref}}$) for all subjects for P, Q, R, S, and T waves.

Lead	Correlation					Difference (ms)				
	P	Q	R	S	T	P	Q	R	S	T
I	0.941	0.975	0.978	0.976	0.739	-4	4	-4	-6	130
II	0.909	0.977	0.978	0.977	0.928	-4	-6	-4	-4	-22
III	0.914	0.978	0.978	0.977	0.685	-4	-2	-4	-2	-22
aVR	0.944	0.977	0.978	0.977	0.633	-4	-10	-4	-6	156
aVL	0.874	0.975	0.978	0.968	0.808	-8	-2	-4	-2	-22
aVF	0.931	0.978	0.978	0.977	0.648	-4	-2	-4	-2	-2
V1	0.946	0.973	0.978	0.970	0.641	-6	-13	-4	-8	-6
V2	0.934	0.977	0.978	0.977	0.742	-4	-4	-4	-14	8
V3	0.928	0.974	0.978	0.976	0.827	-8	-6	-4	-4	24
V4	0.884	0.977	0.978	0.978	0.624	-4	-2	-4	0	-6
V5	0.872	0.976	0.978	0.977	0.632	-4	0	-4	0	4
V6	0.903	0.977	0.978	0.977	0.608	-8	0	-4	2	2
Mean	0.915	0.976	0.978	0.976	0.710	-5	-4	-4	-4	20

Table 4. Data on statistics of subjects S2 and S3 (walking) with coverage: $83.47\% \pm 5.09\%$. Mean correlation and median of time difference ($t_{\text{shirt}} - t_{\text{ref}}$) for all subjects for P, Q, R, S, and T waves.

Lead	Correlation					Difference (ms)				
	P	Q	R	S	T	P	Q	R	S	T
I	0.739	0.901	0.920	0.913	0.580	8	8	2	-4	150
II	0.608	0.921	0.920	0.918	0.600	0	0	2	0	-10
III	0.678	0.921	0.920	0.918	0.439	2	0	2	0	0
aVR	0.739	0.920	0.920	0.918	0.397	2	-2	2	0	140
aVL	0.713	0.910	0.920	0.909	0.384	-20	12	2	14	-20
aVF	0.724	0.920	0.920	0.918	0.440	-2	2	2	2	8
V1	0.701	0.903	0.920	0.895	0.240	-16	2	2	-2	8
V2	0.731	0.893	0.920	0.890	0.274	-12	-2	2	0	30
V3	0.748	0.904	0.920	0.904	0.477	6	2	2	2	24
V4	0.663	0.913	0.920	0.910	0.296	-12	4	2	4	10
V5	0.691	0.912	0.920	0.909	0.346	-10	4	2	4	20
V6	0.704	0.908	0.920	0.907	0.368	-14	2	2	4	20
Mean	0.703	0.910	0.920	0.909	0.403	-6	3	2	2	32

4. Discussion

We have presented a 12-lead textile ECG T-shirt and portable ECG recorder. This device was evaluated using a standard 12-lead Holter as a reference and by conducting a study with healthy volunteers. Three experimental scenarios were devised (lying down, sitting and walking). Evaluation was performed by extracting the RR intervals and comparing the results with the gold standard. Finally, the ECG waves were examined in detail.

The first step was to synchronize the data of both devices. As the devices were not started at exactly the same time, matching was necessary. Moreover, because the sampling rate of 500 Hz produced a different amount of samples for the two devices, this also had to be taken into account. It is most likely that the clocks in the two devices run at a slightly different rate.

By comparing the RR intervals, a very low mean relative error of 0.96% was produced with a coverage of 96.6%. Furthermore, the Bland–Altman diagram (see Figure 9) shows accurate agreement of both systems with a bias of -1.9 ms and 95% limits of agreement of -20.1 ms and -23.9 ms . The bias represents a systematic error between the devices, which equals the possible temporal resolution for 500 Hz (2 ms). Although this is only a small error, it was relevant for the comparison of the ECG waves and the reason why the data were synchronized.

The mean RR interval length was $1.012 \pm 0.071\text{ s}$ for lying, $0.898 \pm 0.079\text{ s}$ for sitting, and $0.800 \pm 0.047\text{ s}$ for walking. Although we had hypothesized that walking would produce more artifacts, the coverage was comparable for all three scenarios. We managed to avoid artifacts by applying sufficiently high contact pressure to the electrodes by putting adjustable Velcro on the back of the T-shirt. At the same time, the pressure of the T-shirt was not so high as to obstruct the subjects' breathing. However, if the T-shirt is planned to be worn by a particular group of patients, other safety measures might be necessary to consider.

One measurement of S1 walking was unsuccessful and consisted mostly of noise. An explanation for this could be the buildup of static charge or triboelectric effects, as explained by Wartzek et al. [28]. According to Wartzek, local triboelectric effects are the source of severe artifacts. They are mainly caused by unmatched electrodes and a bad connection to the DRL. Unmatched electrodes decrease the common mode rejection ratio (CMRR), while the CMRR should be as high as possible for good measurements.

Static effects can be minimized with some arrangements. As little electrode movement as possible is desirable to prevent charges. This is partially accomplished by maintaining sufficient electrode contact. Furthermore, if excess charges occur, a bias resistor in the active electrode allows discharge. Finally, the materials of the contact areas could be selected carefully [14]. An insulated electrode would cause larger electrostatic charges than a metal electrode [28].

After inspection of the RR intervals, the ECG waves were evaluated. The highest correlation was found for the R-waves, which were used to synchronize the data. Furthermore, in every scenario, the Q and S-waves had correlations of over 0.9; in contrast, the T-wave had significantly lower correlations. For lying, the correlation of the P-wave was 0.9198 and the correlation of the T-wave was 0.8171. For sitting, the P-wave still had a correlation of 0.915, but the T-wave only 0.7095. In walking, the P-wave deteriorated to 0.7032 and the T-wave to only 0.4034. This can also be observed in the time differences, which were high for the T-waves. A possible explanation for this is an inaccurate algorithmic determination of the waves. Another reason could be a subpar electrode contact leading to signal deformation, which is determined by the electrode-body interface [14,29]. Sufficient and constant contact pressure is known to be important for textile ECG measurements [1,11,30]. Assuming that the electrodes are the reason for the deformations, the results from Tables 2 and 3 were examined. Lead I, aVR, aVL, V2 and V3 clearly have high time differences. Lead I, aVR and aVL all depend on electrode RA and/or LA. Moreover, V2 and V3 seem to be affected. It is possible that these electrodes did not have sufficient contact pressure.

The coupling of the electrode-skin interface is most likely responsible for these aberrations. The electrode fabric is a silver plated knitted fabric with 99% pure silver. Typically, gel establishes conductive contact and decreases the impedance between the skin and the electrode. For dry contact, this impedance is rather high. That is why active electrodes with voltage followers are used. The input impedance is increased, while the output impedance is decreased [14].

In our experiments, we experienced deteriorated signal quality if the shirt was too loose. In that case, there was not sufficient contact between the skin and the electrode so that the electrode-skin interface became both resistive and capacitive. This combination possibly created a high-pass filter

and caused signal deformation. Further challenges with dry and non-contact electrodes have been discussed by e.g., Chi et al. [9].

The system has not been tested with moisture so far. According to Chi et al., the signal of dry electrodes improves with moisture because it establishes a conductive contact between the electrode and the skin [9]. Additionally, tests with more subjects need to be conducted to ensure long-term functionality and stability. Moreover, adding extra sensors to observe the skin-electrode impedance is recommended, as this will allow to examine morphological differences between the T-shirt ECG.

5. Conclusions

This paper introduces a novel ECG T-shirt for 12-lead measurements with fully active and dry electrodes. A portable 12-lead ECG recorder was developed, which is compatible with the T-shirt. The system is portable and has a battery life of two days. To our knowledge, a 12-lead ECG T-shirt specifically with active electrodes has not been developed before. In a study with three volunteers, the functionality of the device was successfully compared with a commercial device in everyday scenarios. The relative error of the RR intervals was 0.96% with a mean coverage of 96.6%. The P-wave had a correlation of 0.703 for walking subjects, while the T-wave demonstrated lower correlations for all three scenarios (lying: 0.817, sitting: 0.710, walking: 0.403). The other correlations for the P, Q, R, and S-waves were all higher than 0.9. This work shows that a comfortable ECG T-shirt with active electrodes is suitable for 12-lead ECG recordings.

Acknowledgments: This work was funded by the Excellence Initiative of the German federal and state governments (OPBF074).

Author Contributions: W.N., X.Y. and A.B. developed the device. X.Y., W.N. and D.T. conceived and designed the experiments. A.B., X.Y. and D.T. performed the data analysis. A.B., D.T. and S.L. supervised the manuscript writing phase.

Conflicts of Interest: The authors declare no conflict of interest.

Abbreviations

The following abbreviations are used in this manuscript:

ADC	analogue digital converter
aVF	Goldberger lead
aVL	Goldberger lead
aVR	Goldberger lead
CMRR	common mode rejection ratio
CS	chip select line
DRL	driven right leg
ECG	electrocardiography
I	Einthoven I lead
II	Einthoven II lead
III	Einthoven III lead
LA	left arm
LL	left leg
PCB	printed circuit board
RA	right arm
SPI	serial peripheral interface
SPS	samples per second
V1 - V6	Wilson leads
WCT	Wilson central terminal

References

1. Kim, S.; Leonhardt, S.; Zimmermann, N.; Kranen, P.; Kensche, D.; Müller, E.; Quix, C. Influence of contact pressure and moisture on the signal quality of a newly developed textile ECG sensor shirt. In Proceedings of the IEEE 5th International Summer School and Symposium on Medical Devices and Biosensors (ISSS-MDBS 2008), Hong Kong, China, 1–3 June 2008; pp. 256–259.
2. Linz, T.; Kallmayer, C.; Aschenbrenner, R.; Reichl, H. Fully integrated EKG shirt based on embroidered electrical interconnections with conductive yarn and miniaturized flexible electronics. In Proceedings of the BSN 2006: International Workshop on Wearable and Implantable Body Sensor Networks, Cambridge, MA, USA, 3–5 April 2006; pp. 23–26.
3. Ottenbacher, J.; Romer, S.; Kunze, C.; Grosmann, U.; Stork, W. Integration of a Bluetooth Based ECG System into Clothing. In Proceedings of the Eighth International Symposium on Wearable Computers, Arlington, VA, USA, 31 October–3 November 2004; pp. 186–187.
4. Karlsson, J.; Wiklund, U. Wireless Monitoring of Heart Rate and Electromyographic Signals using a Smart T-shirt. In Proceedings of the International Workshop on Wearable Micro and Nanosystems for Personalised Health, Valencia, Spain, 21–23 May 2008.
5. Cardio Leaf. Available online: <http://www.clearbridgevitalsigns.com/shirt.html> (accessed on 19 May 2016).
6. hWear. Available online: <http://www.personal-healthwatch.com/> (accessed on 19 May 2016).
7. Meziane, N.; Webster, J.G.; Attari, M.; Nimunkar, A.J. Dry electrodes for electrocardiography. *Physiol. Meas.* **2013**, *34*, 47–69.
8. Silva, M.; Catarino, A.; Carvalho, H.; Rocha, A.; Monteiro, J.; Montagna, G. Study of vital sign monitoring with textile sensors in swimming pool environment. In Proceedings of the Industrial Electronics Conference (IECON), Porto, Portugal, 3–5 November 2009; pp. 4426–4431.
9. Chi, Y.M.; Jung, T.P.; Cauwenberghs, G. Dry-contact and noncontact biopotential electrodes: Methodological review. *IEEE Rev. Biomed. Eng.* **2010**, *3*, 106–119.
10. Puurtinen, M.M.; Komulainen, S.M.; Kauppinen, P.K.; Malmivuo, J.A.V.; Hyttinen, J.A.K. Measurement of noise and impedance of dry and wet textile electrodes, and textile electrodes with hydrogel. In Proceedings of the Annual International Conference of the IEEE Engineering in Medicine and Biology, New York, NY, USA, 31 August–3 September 2006; pp. 6012–6015.
11. Cömert, A.; Hyttinen, J. Investigating the possible effect of electrode support structure on motion artifact in wearable bioelectric signal monitoring. *Biomed. Eng. Online* **2015**, *14*, 1–18.
12. Meziane, N.; Yang, S.; Shokoueinejad, M.; Webster, J.G.; Attari, M.; Eren, H. Simultaneous comparison of 1 gel with 4 dry electrode types for electrocardiography. *Physiol. Meas.* **2015**, *36*, 513–529.
13. Pani, D.; Dessì, A.; Saenz-Congolo, J.F.; Barabino, G.; Fraboni, B.; Bonfilgio, A. Fully Textile, PEDOT:PSS Based Electrodes for Wearable ECG Monitoring Systems. *IEEE Trans. Biomed. Eng.* **2016**, *63*, 540–549.
14. Sun, Y.; Yu, X. Capacitive Biopotential Measurement for Electrophysiological Signal Acquisition: A Review. *IEEE Sens. J.* **2016**, *16*, 2832–2853.
15. Lim, Y.G.; Kim, K.K.; Park, K.S. ECG measurement on a chair without conductive contact. *IEEE Trans. Biomed. Eng.* **2006**, *53*, 956–959.
16. Leonhardt, S.; Aleksandrowicz, A. Non-contact ECG monitoring for automotive application. In Proceedings of the 5th International Workshop on Wearable and Implantable Body Sensor Networks, Hong Kong, China, 1–3 June 2008; pp. 183–185.
17. Ishijima, M. Monitoring of Electrocardiograms in Bed Without Utilizing Body Surface Electrodes. *IEEE Trans. Biomed. Eng.* **1993**, *40*, 593–594.
18. Lim, Y.G.; Kim, K.K.; Park, K.S. ECG recording on a bed during sleep without direct skin-contact. *IEEE Trans. Biomed. Eng.* **2007**, *54*, 718–725.
19. Wu, K.F.; Zhang, Y.T. Contactless and continuous monitoring of heart electric activities through clothes on a sleeping bed. In Proceedings of the 2008 International Conference on Information Technology and Applications in Biomedicine, Shenzhen, China, 30–31 May 2008; pp. 282–285.
20. Ueno, A.; Yama, Y. Unconstrained monitoring of ECG and respiratory variation in infants with underwear during sleep using a bed-sheet electrode unit. In Proceedings of the 30th Annual International Conference of the IEEE Engineering in Medicine and Biology Society, Vancouver, BC, Canada, 20–24 August 2008; pp. 2329–2332.

21. Kim, K.K.; Lim, Y.K.; Park, K.S. The electrically non-contacting ECG measurement on the toilet seat using the capacitively-coupled insulated electrodes. In Proceedings of the Annual International Conference of the IEEE Engineering in Medicine and Biology Society, Buenos Aires, Argentina, 1–5 September 2004; pp. 2375–2378.
22. Lim, Y.K.; Kim, K.K.; Park, K.S. The ECG measurement in the bathtub using the insulated electrodes. In Proceedings of the Annual International Conference of the IEEE Engineering in Medicine and Biology Society, Buenos Aires, Argentina, 1–5 September 2004.
23. Malmivuo, J.; Plonsey, R. *Bioelectromagnetism: Principles and Applications of Bioelectric and Biomagnetic Fields*; Oxford University Press: Oxford, MI, USA, 2012; pp. 1–506.
24. Sanchez, B.; Praveen, A.; Bartolome, E.; Soundarapandian, K.; Bragos, R. Minimal implementation of an AFE4300-based spectrometer for electrical impedance spectroscopy measurements. *J. Phys.* **2013**, *434*, 012014.
25. Cömert, A.; Hyttinen, J. Impedance spectroscopy of changes in skin-electrode impedance induced by motion. *Biomed. Eng. Online* **2014**, *13*, 149.
26. Tallgren, P.; Vanhatalo, S.; Kaila, K.; Voipio, J. Evaluation of commercially available electrodes and gels for recording of slow EEG potentials. *Clin. Neurophysiol.* **2005**, *116*, 799–806.
27. Bruser, C.; Kortelainen, J.M.; Winter, S.; Tenhunen, M.; Parkka, J.; Leonhardt, S. Improvement of Force-Sensor-Based Heart Rate Estimation Using Multichannel Data Fusion. *IEEE J. Biomed. Health Inform.* **2015**, *19*, 227–235.
28. Wartzek, T.; Lammersen, T.; Eilebrecht, B.; Walter, M.; Leonhardt, S. Triboelectricity in capacitive biopotential measurements. *IEEE Trans. Biomed. Eng.* **2011**, *58*, 1268–1277.
29. Eilebrecht, B.; Czaplik, M.; Wartzek, T.; Schauerte, P.; Leonhardt, S. Analysis of influences on capacitive ECG measurements based on a closed loop model. In Proceedings of the 6th Meeting of the European Study Group on Cardiovascular Oscillations (ESGCO 2010), Berlin, Germany, 12–14 April 2010; pp. 12–15.
30. Reyes, B.A.; Posada-Quintero, H.F.; Bales, J.R.; Clement, A.L.; Pins, G.D.; Swiston, A.; Riistama, J.; Florian, J.P.; Shykoff, B.; Qin, M.; et al. Novel electrodes for underwater ECG monitoring. *IEEE Trans. Biomed. Eng.* **2014**, *61*, 1863–1876.



© 2016 by the authors; licensee MDPI, Basel, Switzerland. This article is an open access article distributed under the terms and conditions of the Creative Commons by Attribution (CC-BY) license (<http://creativecommons.org/licenses/by/4.0/>).